Chemical Communications RSC Publishing

Home Publishing Journals Chemical Communications Advance Articles DOI: 10.1039/b925054a

Chem. Commun., 2010 | DOI: 10.1039/b925054a | Communication

Organometallic control at the nanoscale: a new, one-pot method to decorate a magnetic nanoparticle surface with noble metal atoms[†]

Nabil Atamena [a], Diana Ciuculescu [a], Gilles Alcaraz [a], Alevtina Smekhova [b], Fabrice Wilhelm [b], Andrei Rogalev [b], Bruno Chaudret [a], Pierre Lecante [c], Robert E. Benfield [d] and Catherine Amiens *[a]

[a] *Laboratoire de Chimie de Coordination, CNRS, 205 route de Narbonne, Université de Toulouse, UPS, INPT, LCC, 31077 Toulouse, France. E-mail: amiens@lcc-toulouse.fr; Fax: 33 (0)5 61 55 30 03; Tel: 33 (0)5 31 33 31 82*

[b] *European Synchrotron Radiation Facility, 38043 Grenoble, France. E-mail: rogalev@esrf.fr; Fax: 33 (0)4 76.88 20.20; Tel: 33 (0)4 76.88 20.0*

[c] *Centre d'Elaboration des Matériaux et d'Etudes Structurales, CNRS 29 Rue Jeanne Marvig, BP 4347, 31055, Toulouse, France. E-mail: lecante@cemes.fr; Fax: 33 (0)5 62 25 79 99; Tel: 33 (0)5 62 25 78 51*

[d] *Functional Materials Group, School of Physical Sciences, University of Kent, Canterbury, UK CT2 7NH. E-mail: R.E.Benfield@kent.ac.uk; Tel: 44 (0)1227 823759*

Received (in Cambridge, UK) 30th November 2009 , Accepted 13th January 2010

A novel cascade of reactions is designed to control *in situ* the deposition of noble metal islands (*e.g.* Rh) on top of nanoparticles of a 3d metal (*e.g.* Fe, Co).

Size reduction raises the question of chemical ordering in bimetallic nanoparticles (NPs) of a diameter of a few nanometres. At such a small size, a high tendency towards segregation appears. As the chemical order strongly influences the properties of the particles, both physical and chemical,[1] such segregated bimetallic systems broaden the range of properties that can be accessed by a simple tuning of the composition of alloyed NPs. Segregation of 3d elements at the surface of 4d(5d)–3d bimetallic systems are often reported[2] as expected from thermodynamical considerations.[3] For example, we have recently reported the formation of core–shell Rh/Fe NPs.[4] The formation of these NPs took profit of both the thermodynamic preference for Rh to be at the core of the NP and of the kinetics of the reaction since the chosen Rh precursor ($Rh(allyl)_3$) decomposed much faster than the Fe one ($Fe[N(SiMe_3)_2]_2$). However, depositing a noble metal on top of a 3d one is much more challenging as it leads to a metastable state. Furthermore, redox side reactions between the reduced 3d seeds and the noble metal precursor must be avoided. In this context, organometallic complexes, such as $Rh(allyl)_3$, are promising candidates for precursors of the noble metal. Indeed, as they are not oxidizing, any redox 'transmetallation' process between the precursor and the reduced 3d seeds is prevented. Last, mild conditions need to be used to impose a precise chemical order since atom diffusion is very easy at this size.

Borohydrides ($NaBH_4$, $LiBHEt_3$, …) and H_2 are the most widely used reducing agents to produce metal NPs. Recently, the use of amine–borane adducts has been reported as an elegant alternative to borohydrides.[5,6] Especially, it was observed that amine–borane derivatives react instantaneously, even at very low temperatures, with amido metal complexes with production of the metal and H_2, when the metal hydrides are thermodynamically unstable which is the case *e.g.* for iron or cobalt.[7] From these results we inferred that, as H_2 is often used to reduce noble metal organometallic precursors in mild conditions, a novel cascade of reactions could be designed to deposit a noble metal on top of metal NPs prepared through amine–borane reduction (which would thus play the role of seeds).

Here we report the selective one-pot deposition of Rh on Fe (or Co) nanoparticles using a novel organometallic control.

We first chose the bimetallic $Fe_{85}Rh_{15}$ system as suitable complexes ($Fe[N(SiMe_3)_2]_2$ and $Rh(\eta^3\text{-}C_3H_5)_3$) where described in the literature[8,9] and well-defined NPs of identical composition but reverse chemical order were already published and could be used as a comparison point.[4] Furthermore, Rh is a costly but very active catalyst.[10] Decorating Fe NPs with Rh atoms could thus lead to low cost, magnetically recoverable, catalytic platforms of high efficiency.[11]

Reaction at low temperature of 3.4 equiv. $iPr_2NH.BH_3$,[12] with 1.7 equiv. $Fe[N(SiMe_3)_2]_2$, 0.3 equiv. $Rh(\eta^3\text{-}C_3H_5)_3$ and 1 equiv. of tetramethylpiperidine as a stabilizing agent in heptane afforded first H_2 evolution and, after 12 h, a black solution. From evaporation of the solvent, the NPs were recovered as a black powder (**1**). TEM study evidences NPs, with average diameters of 1.7 nm (σ = 0.2) according to a Gaussian fit of the size distribution. A typical image is given in Fig. 1. Monometallic NPs were also prepared from pure $Fe[N(SiMe_3)_2]_2$ (**2**) and $Rh(\eta^3\text{-}C_3H_5)_3$ (**3**) solutions for comparison sake. The Fe NPs in **2** display an average size of 1.7 nm (σ = 0.3) (ESI†). The volatile constituents of the reacting medium were recovered in a trap and analysed by ^{11}B and ^1H NMR. The by-products of the reaction were found to be hexamethyldisilazane, and the amino–borane derivative $iPr_2N\text{–}BH_2$ which was recovered quantitatively. When the Rh precursor alone was reacted with the amine–borane complex, the reaction was very slow. No change in the ^1H NMR spectrum could be evidenced before 2 h of reaction. Some NPs of average size 1.9 nm (σ = 0.7) could be evidenced by TEM after 12 h of reaction (ESI†). This confirms that only the Fe precursor reacts with the amine–borane complex during preparation of **1**.

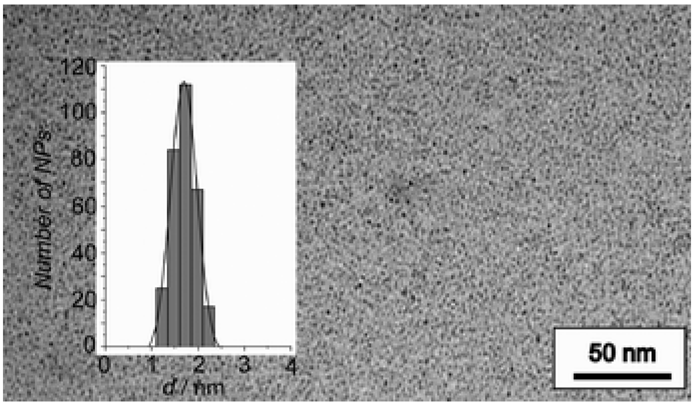

Fig. 1 TEM image, size histogram for $Fe_{85}Rh_{15}$ NPs (sample **1**).

Given the small size of the NPs, direct imaging of the location of Fe and Rh atoms inside the NPs could not be achieved *via* EFTEM or related techniques. The location of Rh atoms was thus investigated by combining wide-angle X-Ray scattering (WAXS), EXAFS, XMCD measurements and IR spectroscopy.

Fig. 2 displays the experimental radial distribution functions (RDF) obtained by WAXS for **1–3**, as well as those generated from model clusters and from FeRh NPs of identical composition with Rh atoms buried in the core (**4**) from ref. 4. The RDF for **4** was reported to result from a Rh fcc core surrounded by an amorphous Fe layer due to lattice mismatch and geometric constraints, and shown to contain mainly fcc features. In contrast, the NPs from **1** and **2** adopt a polytetrahedral packing, supporting the hypothesis of an iron polytetrahedral core. Rh atoms either also adopt a polytetrahedral packing, or form an amorphous rhodium shell, while they clearly adopt a fcc packing in **3**.

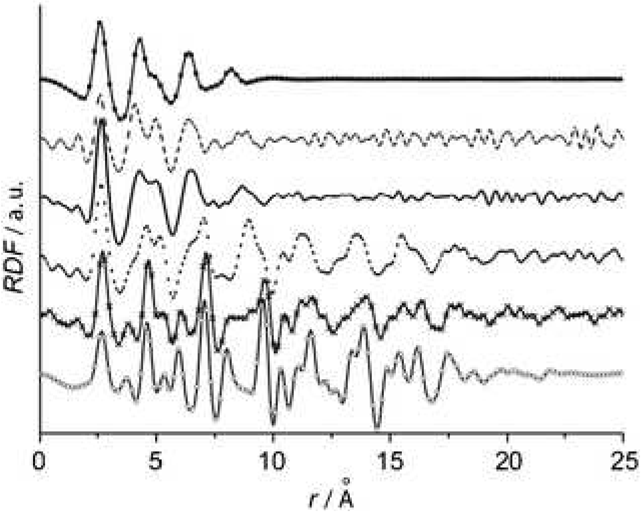

Fig. 2 RDF for, from top to bottom: a polytetrahedral packing,[13] Fe NPs (**2**), $Fe_{85}Rh_{15}$ NPs (**1**), $Rh_{15}Fe_{85}$ NPs (**4**), Rh NPs (**3**) and a model fcc cluster.[13]

Next, XAS measurements were carried out at Fe and Rh K edges. At the absorption edge, the spectra superpose perfectly on those of the corresponding metal foils demonstrating the absence of oxidation (ESI†). This rules out any transmetallation process between the Fe initial seeds and the Rh organometallic precursors, and any adventitious oxidation of the final NPs. The fine structures at both edges are different from that of the reference metal foils showing a different atomic packing, as expected from NPs of polytetrahedral packing (ESI†). RDF obtained from the EXAFS data are reported in Fig. 3. No phase correction was applied in this preliminary analysis. At Rh K-edge, distances in **1** are much more dispersed than in **3** (fcc Rh NPs) and significantly shifted towards low values as expected for a polytetrahedral environment. By comparison with the RDF of **3** (pure Rh NPs) the right hand shoulder has been attributed to Rh–Rh bonds.

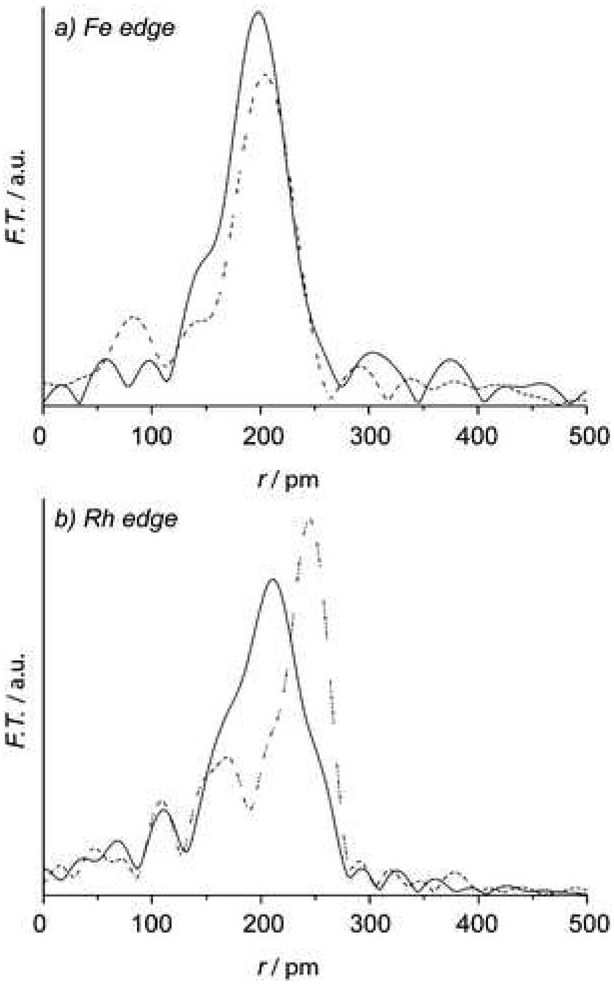

Fig. 3 RDF of the EXAFS signal for: (a) $Fe_{85}Rh_{15}$ NPs (**1**) (solid line) and Fe NPs (**2**) (dotted line), (b) **1** (solid line) and Rh NPs (**3**) (dotted line).

The main peak would thus be indicative of Rh–Fe bonds. It is noteworthy that XANES spectra of Rh atoms are strongly affected upon air exposure (ESI†) as expected for atoms localised at the surface. This is not the case for **4**[4] for which Rh atoms are buried in the core of the NP. At Fe K-edge, the main distance has been attributed to the Fe–Fe distance as it was the only one present in **2**. It is not clear if the peak contains Fe–Rh contributions.

To further ascertain the presence of Rh in the vicinity of Fe atoms, we carried out XMCD measurements at Rh $L_{2,3}$ edges. From the ± polarisation curves, a significant dichroic signal could be extracted, from which the magnetic moment for Rh atoms was calculated: $0.63\mu_B$ per atom. This value agrees well with those reported in the literature for Rh atoms deposited on Fe surfaces.[14] It is noteworthy that this value is lower than that reported for the system of reverse chemical order ($0.72\mu_B$ per atom).[15] As Rh generally polarizes more when embedded inside a 3d transition metal matrix,[16] this result is a further confirmation of the control we have on the chemical order.

Last, a chemical probe, CO was used to investigate the surface of the NPs in **1**, **2** and **3**. The IR spectra of the NPs submitted to 1 bar CO are reported in the ESI.† Absorption bands corresponding to CO in atop configuration are observed in each case, located at 1952 cm^{-1} for pure Fe NPs (**2**), and 2005 cm^{-1} for pure Rh NPs (**3**) while two peaks are observed for FeRh NPs at 1996 and 1975 cm^{-1} which we attribute to CO adsorbed on Rh and Fe atoms, respectively, evidencing a mixed surface.

IR spectroscopy, XAS and XMCD measurements thus point to Rh atoms located at the surface of the NPs.

To evidence the versatility of our concept we reacted the analogous Co amido complex $Co[N(SiMe_3)_2]_2$,[8] and $Rh(\eta^3\text{-}C_3H_5)_3$ in the same conditions. Combining TEM, WAXS, XAS and XMCD, we observed 1.8 nm large NPs of polytetrahedral packing, Rh–Rh, Rh–Co and Rh-ligand distances and a dichroic signal at the Rh L_2 edge, here again in agreement with the deposition of Rh atoms at the NPs surface (see ESI†).

Based on the NMR study it is clear that the amine–borane does not react as a simple hydride reducing agent, as is the case when engaged in the synthesis of *e.g.* gold NPs.[5] The quantitative formation of amino–borane demonstrates a dehydrogenation process. The NPs being magnetic the reaction could not be further studied by NMR, and we can only suggest the mechanism depicted on Fig. 4. Given the atomic Rh : M ratios used here (15 : 85 in **1**, 25 : 75 in **2**) the H_2 quantity produced in the first step of the reaction is sufficient to ensure complete reduction of the Rh complex in the second step. Indeed the proposed mechanism suggests a maximum Rh : Fe ratio of 40 : 60. It also suggests that the nature of the amine borane reactant determines the nucleation step, and consequently the final size of the NPs. Tuning the reactivity of the amine–borane complex should thus enable tuning the size of the NPs.

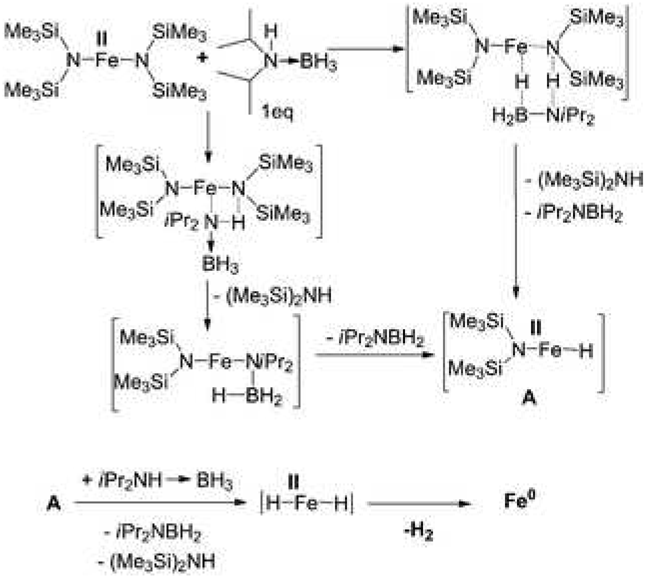

Fig. 4 Mechanistic steps proposed for the reaction between the Fe amido complex and the amine–borane complex.

The main purpose of this work was to develop a new tool for depositing a controlled amount of noble metal on top of a 3d NP. We have shown that the one-pot reaction between $iPr_2NH{\cdot}BH_3$, $Rh(allyl)_3$ and $M[N(SiMe_3)_2]_2$ (M = Co or Fe) affords NPs with a surface decorated with Rh. The cascade of reactions developed (formation of the Fe or Co seeds with production of dihydrogen, then hydrogenation of the Rh complex) timely separates the two reduction steps insuring *in situ* the exclusive deposition of the Rh atoms on top of the Fe seeds. It also provides a cost effective synthesis route. This synthetic method should apply to other bimetallic systems, as long as amido and olefinic or alkyl/aryl complexes exist for the two metals envisaged, thus extending the scope of available bimetallic systems. It is important to realize that depositing a noble metal on top of a zerovalent 3d NP, without altering it, is highly challenging. Especially side reactions between the 3d NP and the noble metal precursor must be avoided. In this context, the use of organometallic complexes which are much less oxidizing than salts proves to be a huge advantage.

We thank the EC for support through MRTN CT-2004-0055667 and FP7/2007-2013 (grant no. 226716 at the light source facilities DORIS III, HASYLAB/DESY). DESY is a member of the Helmholtz Association (HGF). We would like to thank E. Welter for assistance on beamline C. We acknowledge the European Synchrotron Radiation Facility for provision of synchrotron radiation facilities (beamline ID-12, project HE-3006). This work benefited from a financial support from the Agence Nationale pour la Recherche (ANR-09-BLAN-0002-01).

Notes and references

1 O. Margeat, D. Ciuculescu, P. Lecante, M. Respaud, C. Amiens and B. Chaudret, *Small*, 2007,

3(3), 451–458 [Links]; C. Bergounhou, C. Blandy, R. Choukroun, P. Lecante, C. Lorber and J.-L. Pellegatta, *New J. Chem.*, 2007, **31**(2), 218–223 [Links].

2 T. Teranishi and M. Miyake, *Chem. Mater.*, 1999, **11**, 3414 [Links]; N. S. Sobal, U. Ebels, H. Mohwald and M. Giersig, *J. Phys. Chem. B*, 2003, **107**, 7351 [Links]; X. Teng, D. Black, N. J. Watkins, Y. Gao and H. Yang, *Nano Lett.*, 2003, **3**, 261 [Links]; M. Delalande, P. R. Marcoux, P. Reiss and Y. Samson, *J. Mater. Chem.*, 2007, **17**, 1579 [Links]; I.-C. Chiang and D.-H. Chen, *Adv. Funct. Mater.*, 2007, **17**, 1311 [Links].

3 L.-L. Wang and D. D. Johnson, *J. Am. Chem. Soc.*, 2009, **131**, 14023 [Links].

4 D. Ciuculescu, C. Amiens, M. Respaud, A. Falqui, P. Lecante, R. E. Benfield and B. Chaudret, *Chem. Mater.*, 2007, **19**, 4624 [Links].

5 S. Peng, Y. Lee, C. Wang, H. Yin, S. Dai and S. Sun, *Nano Res.*, 2008, **1**, 229.

6 N. Zheng, J. Fan and G. D. Stucky, *J. Am. Chem. Soc.*, 2006, **128**, 6550 [Links]; S. Maksimuk, S. Yang, Z. Peng and H. Yang, *J. Am. Chem. Soc.*, 2007, **129**, 8684 [Links].

7 A. Glaria, *PhD Thesis*, Université Paul-Sabatier, Toulouse, 2007.

8 R. A. Andersen, K. Faegri, J. C. Green, A. Haaland, M. F. Lappert, W.-P. Leung and K. Rypdal, *Inorg. Chem.*, 1988, **27**, 1782 [Links].

9 R. Beckhaus, in *Synthetic Methods of Organometallic and Inorganic Chemistry*, ed. W. A. Herrmann, New York, 2000, vol. 9.

10 L. Barthe, A. Denicourt-Nowicki, A. Roucoux, K. Philippot, B. Chaudret and M. Hémati, *Catal. Commun.*, 2009, **10**, 1235 [Links].

11 H. Durr and J. Phillips, *J. Catal.*, 1990, **126**, 619 [Links].

12 I. G. Green and B. P. Roberts, *J. Chem. Soc., Perkin Trans. 2*, 1986, 1597 [Links].

13 F. Dassenoy, M.-J. Casanove, P. Lecante, M. Verelst, E. Snoeck, A. Mosset, T. O. Ely, C. Amiens and B. Chaudret, *J. Chem. Phys.*, 2000, **112**, 8137 [Links].

14 L. Zhong and J. Freeman, *J. Appl. Phys.*, 1997, **81**, 3890 [Links].

15 A. Smekhova, D. Ciuculescu, P. Lecante, F. Wilhelm, C. Amiens, A. Rogalev and B. Chaudret, *IEEE Trans. Magn.*, 2008, **44**, 2776 [Links].

16 M. Muñoz-Navia, J. Dorantes-D'avila, D. Zitoun, C. Amiens, B. Chaudret, M.-J. Casanove, P. Lecante, N. Jaouen, A. Rogalev, M. Respaud and G. M. Pastor, *Faraday Discuss.*, 2008, **138**, 181 [Links].

Footnote

† Electronic supplementary information (ESI) available: Full experimental details, TEM images, size histograms, XAS spectra, IR spectra, data for the CoRh system. See DOI: 10.1039/b925054a

---